Clim Dyn (2014) 43:193–207
DOI 10.1007/s00382-013-1820-y

Cross-season relation of the South China Sea precipitation variability between winter and summer

Renguang Wu · Gang Huang · Zhencai Du · Kaiming Hu

Received: 26 February 2013 / Accepted: 28 May 2013 / Published online: 5 June 2013

Abstract The present study reveals cross-season connections of rainfall variability in the South China Sea (SCS) region between winter and summer. Rainfall anomalies over northern South China Sea in boreal summer tend to be preceded by the same sign rainfall anomalies over southern South China Sea in boreal winter (denoted as in-phase relation) and succeeded by opposite sign rainfall anomalies over southern South China Sea in the following winter (denoted as out-of-phase relation). Analysis shows that the in-phase relation from winter to summer occurs more often in El Niño/La Niña decaying years and the out-of-phase relation from summer to winter appears more frequently in El Niño/La Niña developing years. In the summer during the El Niño/La Niña decaying years, cold/warm and warm/cold sea surface temperature (SST) anomalies develop in tropical central North Pacific and the North Indian Ocean, respectively, forming an east–west contrast pattern. The in-phase relation is associated with the influence of anomalous heating/cooling over the equatorial central Pacific during the mature phase of El Niño/La Niña events that suppresses/enhances precipitation over southern South China Sea and the impact of the above east–west SST anomaly pattern that reduces/increases precipitation over northern South China Sea during the following summer. The impact of the east–west contrast SST anomaly pattern is confirmed by numerical experiments with specified SST anomalies. In the El Niño/La Niña developing years, regional air-sea interactions induce cold/warm SST anomalies in the equatorial western North Pacific. The out-of-phase relation is associated with a Rossby wave type response to anomalous heating/cooling over the equatorial central Pacific during summer and the combined effect of warm/cold SST anomalies in the equatorial central Pacific and cold/warm SST anomalies in the western North Pacific during the mature phase of El Niño/La Niña events.

Keywords Cross-season precipitation connection · The South China Sea · El Niño/La Niña · SST anomaly pattern · Air-sea interaction

R. Wu (✉)
Institute of Space and Earth Information Science, Fok Ying Tung Remote Sensing Science Building, The Chinese University of Hong Kong, Shatin, NT, Hong Kong SAR, China
e-mail: renguang@cuhk.edu.hk

G. Huang · Z. Du · K. Hu
Institute of Atmospheric Physics, Chinese Academy of Sciences, Beijing, China

1 Introduction

The South China Sea is located between the Pacific and Indian Oceans and to southeast of the Asian land. On one hand, climate variability in the South China Sea region is influenced by anomalous states of the tropical Indian and Pacific Oceans (Wang et al. 2002, 2006; Xie et al. 2003). On the other hand, anomalous state of the South China Sea can affect East and Southeast Asian climate (Tomita and Yasunari 1996; Zhou et al. 2010). Thus, investigating the climate variability and predictability in the South China Sea region can help to improve the understanding of the influences of tropical Pacific and Indian Oceans on East and Southeast Asian climate.

As demonstrated by previous studies, the El Niño-Southern Oscillation (ENSO) induced short-term climate signals display regional features and evolve with season (Wang et al. 2000, 2003; Wu et al. 2003). For example, Wu et al. (2003) showed that ENSO-induced rainfall anomalies

in China are positive in southern China during fall and winter and positive rainfall anomalies extend to central China in the following summer. Following the phase change of ENSO, anomalous anticyclonic winds move eastward and northward from fall to winter, spring and summer over the North Indian Ocean and the western North Pacific. As the South China Sea has a large meridional extension from near the equator to about 25°N, ENSO-related climate anomalies in the South China Sea are expected to change with the phase of ENSO and thus may depend upon the season. In particular, climate anomalies in the South China Sea region may display different features in winter and summer. One issue is whether there is a cross-season connection of climate anomalies in the South China Sea region. In the present study, we particularly focus on the connection of winter and summer rainfall variability in the South China Sea region. This distinguishes from previous studies that are mostly concerned with climate anomalies in an individual season. Such cross-season connection, if present, will provide useful information for climate predictability.

While ENSO is often considered as a dominant factor for climate variability in tropical regions, such as the South China Sea, other factors, such as regional sea surface temperature (SST) anomalies, may play a role in the South China Sea climate variability as well. For example, Yang et al. (2007) and Xie et al. (2009) showed the role of the North Indian Ocean SST anomalies in an anomalous lower-level anticyclone over the western North Pacific in summer. Wu et al. (2012) indicated the impact of the SST anomalies in the tropical southeast Indian Ocean on vertical motion over the South China Sea in summer. Thus, another issue to be addressed in the present study is what roles of regional SST anomalies play in the cross-season connection of the South China Sea climate anomalies.

In the following, we describe the datasets and model used in the present study in Sect. 2. The leading modes of winter and summer rainfall anomalies and their relations are presented in Sect. 3. Section 4 investigates the winter-to-summer rainfall relation. Section 5 addresses the summer-to-winter rainfall relation. A summary is given in Sect. 6 along with discussions.

2 Datasets and model

2.1 Datasets

The present study uses monthly mean rainfall from version 2 of the Global Precipitation Climatology Project (GPCP) (Adler et al. 2003). The GPCP rainfall is obtained through anomalous ftp at ftp://precip.gsfc.nasa.gov/pub/gpcp-v2/psg/. This dataset is on a 2.5° × 2.5° grid and is available starting from January 1979.

The SST used in the present study is the NOAA Extended Reconstruction monthly mean SST version 3 (ERSST3) (Smith et al. 2008). ERSST3 is provided by NOAA's Office of Oceanic and Atmospheric Research (OAR) Earth System Research Laboratory (ESRL) Physical Science Division (PSD), Boulder, Colorado, obtained from the website at http://www.esrl.noaa.gov/psd/data/gridded/data.noaa.ersst.html. This SST dataset is available on a 2° × 2° grid from 1,854 to present.

We use monthly mean surface shortwave radiation, longwave radiation, latent heat flux, sensible heat flux, and wind speed from the National Oceanography Center, Southampton (NOCS) flux dataset version 2.0 (Berry and Kent 2009). NOCS version 2.0 is constructed using ship data only from the International Comprehensive Ocean–Atmosphere Dataset (ICOADS) through optimal interpolation. This dataset has a spatial resolution of 1° × 1° and covers the period 1973–2009.

The present study uses monthly mean winds at 850 hPa from the National Centers for Environmental Prediction–Department of Energy (NCEP–DOE) Reanalysis version 2 (Kanamitsu et al. 2002) on a regular 2.5° × 2.5° grid for the period 1979–2008. The reanalysis product is provided by the NOAA–Cooperative Institute for Research in Environmental Sciences (CIRES) Climate Diagnostics Center, Boulder, Colorado, and is obtained through anomalous ftp at ftp://ftp.cdc.noaa.gov/.

2.2 Model

The present study uses the Community Atmosphere Model Version 3.1 (CAM3.1) at T42 resolution in the horizontal and with 23 sigma levels in the vertical. For descriptions of the model details, refer to Collins et al. (2006). A long-term control integration over 50 years is made with climatological SST specified in the global oceans. Sensitivity experiments are conducted with SST anomalies added in the concerned regions to investigate the roles of regional SST anomalies. These sensitivity experiments start from initial states of the control integration. The differences of the atmospheric states in these sensitivity experiments from those in the control integration are considered as response of the atmosphere to the specified SST anomalies.

3 Leading modes of winter and summer rainfall anomalies and their relations

An empirical orthogonal function (EOF) analysis is performed for winter (December-January–February or DJF in short) and summer (June–July–August or JJA in short) rainfall anomalies. Here, December belongs to the previous year. In performing the EOF analysis, the rainfall anomalies have been interpolated to 1° × 1° grids for a better coverage of the South

China Sea domain. In winter, the leading and second modes account for about 69.2 and 9.9 % of the total variance, respectively. In summer, the leading and second modes explain about 33.7 and 20.3 % of the total variance, respectively. Thus, the leading mode is separated from the other modes according to North et al. (1982). Figure 1a, b show the distribution of the spatial loading of the leading modes in winter and summer, respectively. The corresponding time series of the leading modes are shown in Fig. 1c.

In winter, large loading is seen over southeastern South China Sea (Fig. 1a). In summer, large positive loading appears over northeastern South China Sea and large negative loading is confined to the coast of Borneo (Fig. 1b). The above distributions indicate that the leading mode in winter features rainfall variability in southern South China Sea and that in summer features rainfall variability in northern South China Sea. Indeed, the correlation coefficient between the winter leading mode time series and area-mean winter rainfall in the region of 2.5°–12.5°N, 107.5°–117.5°E (box in Fig. 1a) is as high as 0.99 and that between the summer leading mode time series and area-mean summer rainfall in the region of 12.5°–22.5°N, 110°–120°E (box in Fig. 1b) is as high as 0.94. Thus, the leading modes can represent well the rainfall variability over southern South China Sea in winter and northern South China Sea in summer, respectively.

The correlation coefficient between the time series of winter and summer leading modes is +0.37 for the period 1979–2010. The correlation coefficient between the two leading mode time series with the summer one leading the winter one is −0.44. The two correlation coefficients are significant at the 95 % confidence level according to the Student *t* test. This indicates a tendency for rainfall anomalies over southern South China Sea in winter to be followed by the same sign rainfall anomalies over northern South China Sea in the following summer and a tendency for rainfall anomalies over northern South China Sea in summer to be followed by opposite sign rainfall anomalies over southern South China Sea in the succeeding winter. For convenience, the former tendency is denoted as in-phase relation and the latter tendency is denoted as out-of-phase relation hereafter. Note that the above relations involve a change in the location of large rainfall anomalies. The time series display large amplitudes in 1983 and 1998

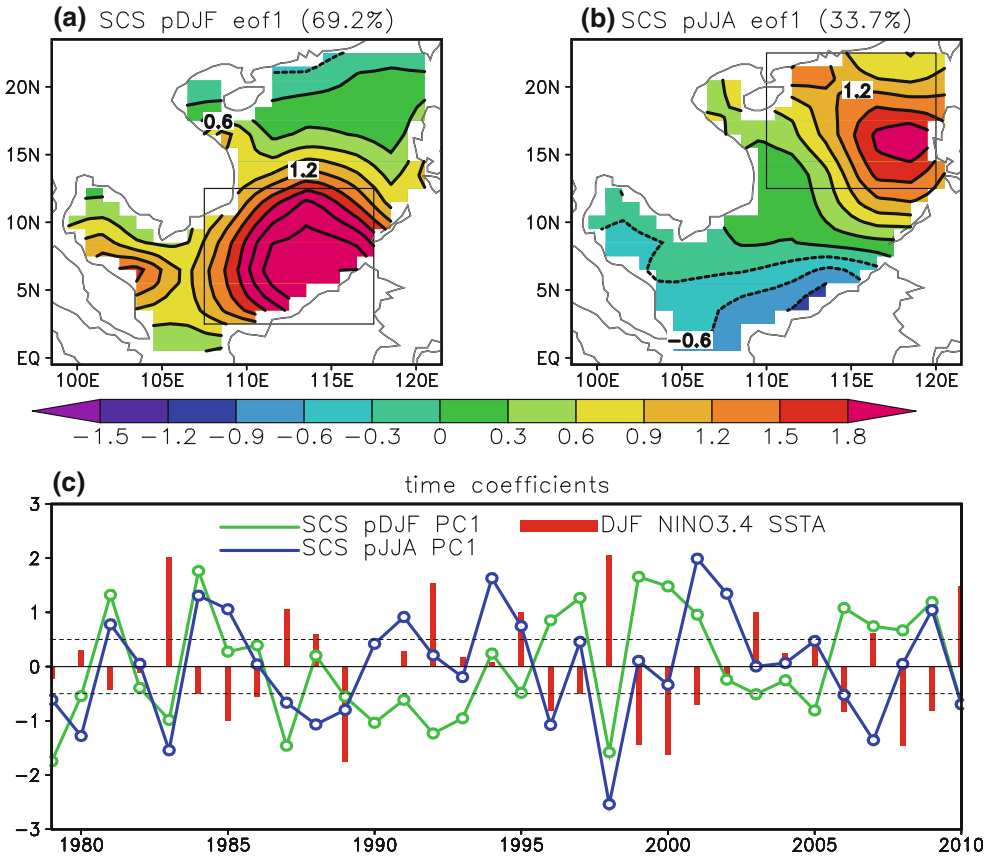

Fig. 1 Distribution of spatial loading of the leading mode of precipitation anomalies in DJF (**a**) and JJA (**b**) and the corresponding time series of the leading modes (*curves*) and DJF NINO3.4 SST anomalies (*bar*) (**c**). The contour interval is 0.3 in (**a**) and (**b**). The boxes in (**a**) and (**b**) denote the regions for calculation of area-mean rainfall

(Fig. 1c). This indicates a large contribution to the correlation from 1982/83 and 1997/98 events.

The above relations are confirmed by the correlation of grid-point rainfall anomalies in the preceding and succeeding winters with the summer leading mode time series. In the preceding winter, significant positive correlation is seen in southern South China Sea (Fig. 2a). In the succeeding winter, significant negative correlation is observed in southern South China Sea (Fig. 2b). Similar correlation distribution is obtained when the correlation is calculated with reference to area-mean summer rainfall over the region of 12.5°–22.5°N, 110°–120°E (Fig. 2c, d) where the largest loading is seen in the summer leading mode.

Detailed examination of the leading mode time series indicates both in-phase and out-of-phase relations from winter to summer and from summer to winter. Table 1 lists the in-phase and out-of-phase relation years during the analysis period based on the criterion of 0.5 standard deviation of the time series of the leading modes. From winter to summer, there are 11 in-phase relation cases and 6 out-of-phase relation cases, respectively. From summer to winter, there are 10 out-of-phase relation cases and 5 in-phase relation cases, respectively. Thus,

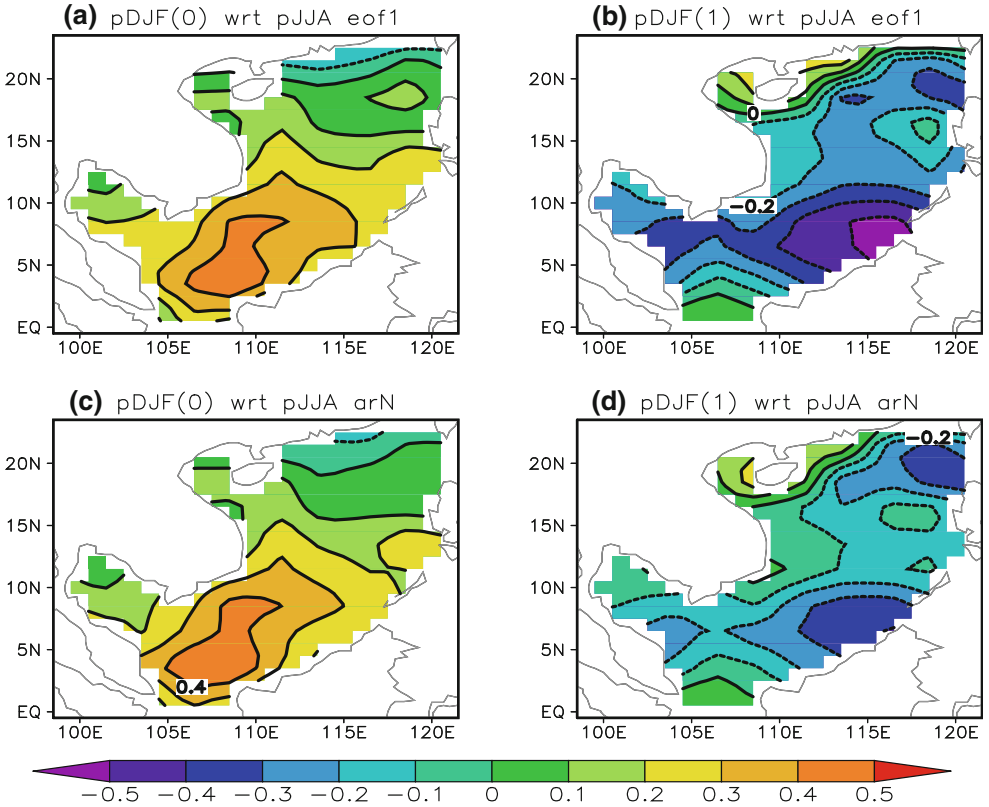

Fig. 2 Distribution of correlation coefficient of grid-point precipitation anomalies in preceding DJF (**a**) and succeeding DJF (**b**) with respect to the time series of the leading mode of JJA precipitation anomalies. **c**, **d** are similar to (**a**) and (**b**) except with respect to area-mean JJA precipitation anomalies over northern South China Sea (12.5°–22.5°N, 110°–120°E). The contour interval is 0.1

Table 1 Years of in-phase and out-of-phase relations between winter and summer

	Winter to summer	Summer to winter
In-phase relation	1979−, 1980−, 1981+, **1983−**, **1984+**, **1987−**, 1989−, **1998−**, **2001+**, **2009+**, **2010−**	1979−, 1988−, 1989−, 1995+, 2005+
Out-of-phase relation	1991−, 1995−, 1996+, 2005−, 2006+, 2007+	1980−, **1983–**, **1991+**, **1994+**, **1996−**, **1998−**, **2002+**, 2006−, **2007−**, **2009+**

The "−"/"+" signs denote negative/positive winter rainfall anomalies in southern South China Sea for in-phase relation from winter to summer or negative/positive summer rainfall anomalies in northern South China Sea for out-of-phase relation from summer to winter. Bold values denote El Niño/La Niña decaying years for in-phase relation from winter to summer with opposite sign DJF NINO3.4 SST and southern South China Sea rainfall anomalies and El Niño/La Niña developing years for out-of-phase relation from summer to winter with the same sign JJA NINO3.4 SST and northern South China Sea rainfall anomalies. Underlined values denote El Niño/La Niña decaying years and El Niño/La Niña developing years that do not fit the above categories

there are more in-phase relation years than out-of-phase relation years from winter to summer and more out-of-phase than in-phase relation years from summer to winter. This contrast is consistent with the result of correlation analysis.

The cross-season relation provides a source of predictability for rainfall anomalies over the South China Sea. One question is what contributes to the cross-season connection of the South China Sea rainfall variability. This question is addressed in the following sections. Understanding the factors for the cross-season connection can help to unravel the source of predictability of the South China Sea climate.

4 In-phase relation from winter to summer

Among the 11 in-phase relation cases, 7 cases (1983, 1984, 1987, 1998, 2001, 2009, 2010) occurred in El Niño and La Niña decay years (Fig. 1c). This indicates that ENSO is an important factor for the in-phase relation from winter to summer. Indeed, the correlation coefficients between the winter and summer leading mode time series and DJF NINO3.4 (5°S–5°N, 170°–120°W) SST anomalies are −0.66 and −0.37, respectively, both of which are significant at the 95 % confidence level according to the Student *t* test. In this study, El Niño and La Niña events are defined following the Climate Prediction Center (CPC) of National Ocean and Atmosphere Administration (NOAA). Specifically, cold and warm episodes are defined when the threshold ±0.5 °C is met for a minimum of 5 consecutive over-lapping seasons (http://www.cpc.ncep.noaa.gov/products/analysis_monitoring/ensostuff/ensoyears.shtml).

To understand the processes leading to the in-phase relation, we examine the evolution of composite anomalies from winter to summer. The composite has been made for all the 11 cases, the 7 ENSO-related cases, and the 4 non-

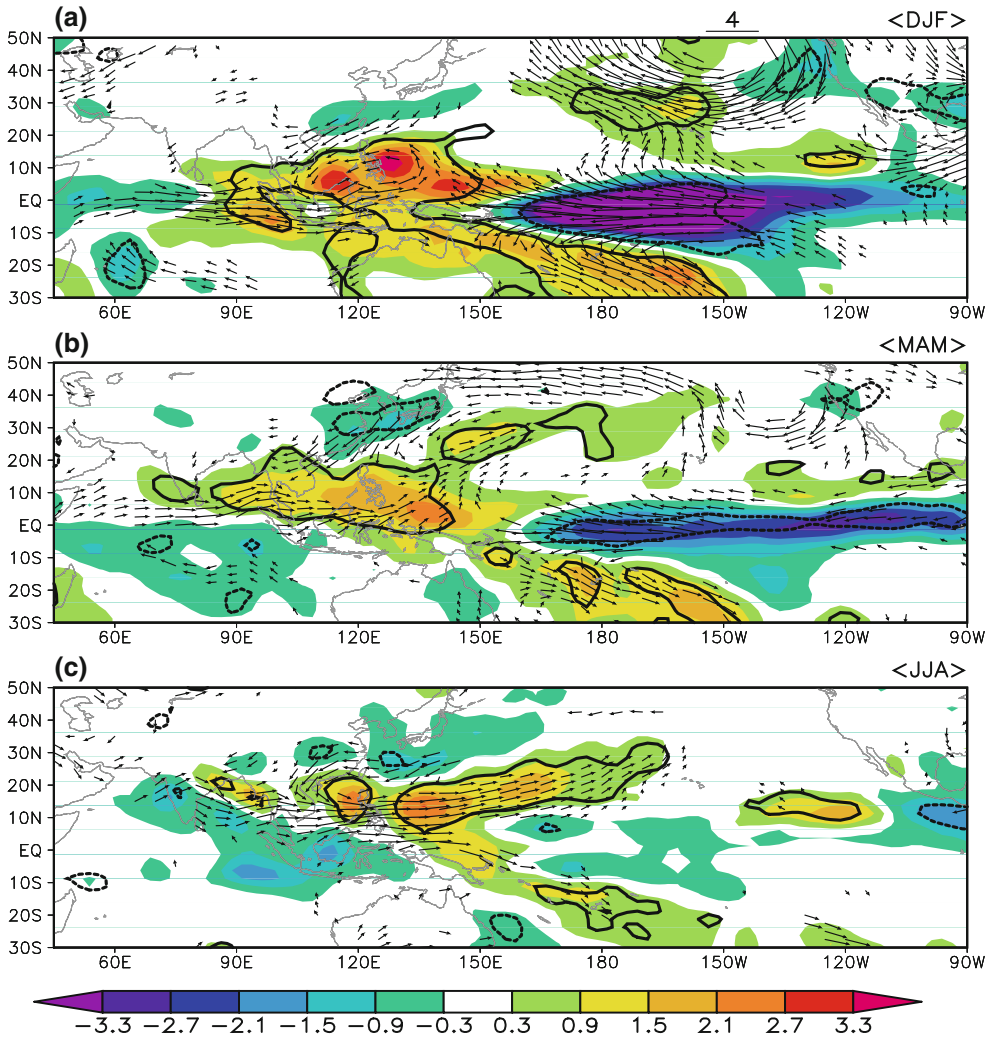

Fig. 3 Composite anomalies of precipitation (*shading*, unit: mm/day) and 850 hPa wind (*vector*, unit: m/s) in DJF (**a**), MAM (**b**), and JJA (**c**) for ENSO-related winter to summer in-phase relation cases. The wind scale is shown at the top. Thick contours denote regions where the composite precipitation anomalies are significant at the 95 % confidence level according to one sample *t* test. Only wind anomaly vectors that are significant at the 95 % confidence level are shown

ENSO-related cases. Here, we focus on analyzing the 7 ENSO-related case composite. The 11 case composite displays features similar to the 7 ENSO-related case composite but with lower level of statistical significance in the composite fields. Figure 3 displays the composite precipitation and 850 hPa wind anomalies from winter to summer for the 7 ENSO-related cases. Figure 4 is similar to Fig. 3 except for SST anomalies. In constructing the composite, we have reversed signs of anomalies for cases with negative time coefficient values. The statistical significance is determined based on one sample t test.

The temporal evolution of composite wind, precipitation, and SST anomalies is typical of that in La Niña decaying years (Wang et al. 2003; Wu et al. 2003). In winter, there are westerly wind anomalies over the equatorial Indian Ocean, easterly wind anomalies over the equatorial western and central Pacific Ocean, and an anomalous cyclone over the South China Sea and the Philippine Sea (Fig. 3a). Precipitation anomalies are negative over the equatorial Pacific, positive over eastern Indian Ocean, southern South China Sea, and the Philippine Sea. At this time, precipitation anomalies are small over northern South China Sea. The wind and precipitation anomalies feature a response to negative SST anomalies in the equatorial central and eastern Pacific (Fig. 4a). Anomalous cooling associated with negative SST anomalies in the equatorial central Pacific leads to compensating upward motion and lower-level cyclonic winds over the South China Sea and the Philippine Sea (Wang et al. 2000). The regional warm SST anomalies over tropical western

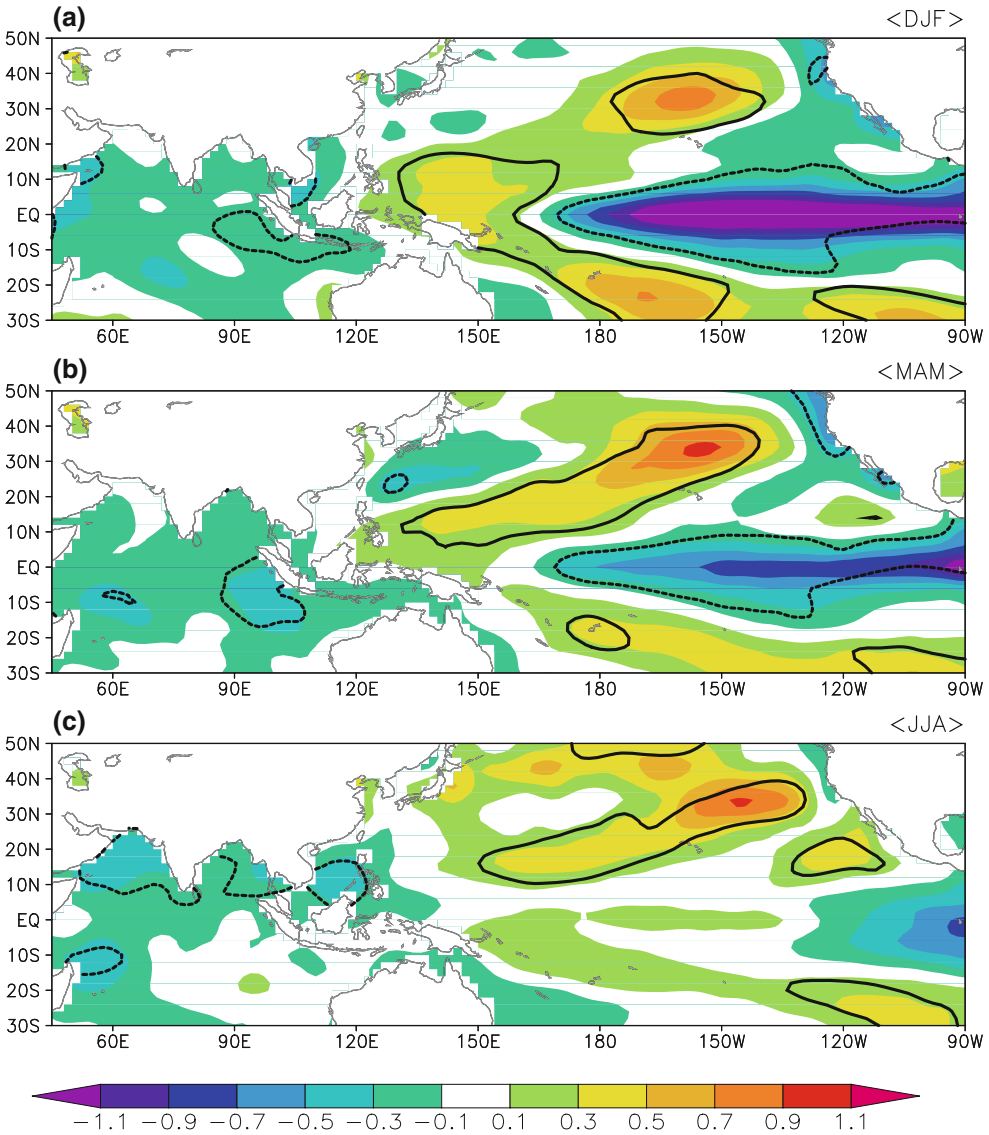

Fig. 4 Composite anomalies of SST (°C) in DJF (**a**), MAM (**b**), and JJA (**c**) for ENSO-related winter to summer in-phase relation cases. Thick contours denote regions where the composite SST anomalies are significant at the 95 % confidence level according to one sample t test

North Pacific may also contribute to the precipitation increase through modulating the convective stability and lower-level convergence (Wu and Wang 2000).

In spring (March–April–May or MAM in short), equatorial central Pacific SST anomalies weaken (Fig. 4b), so do precipitation and lower-level wind anomalies (Fig. 3b). The anomalous lower-level cyclone over the South China Sea and the Philippine Sea migrates eastward. The positive SST anomalies in southern Philippine Sea shrink in areal coverage. In summer, equatorial Pacific SST anomalies become weak (Fig. 4c), so do the lower-level wind and precipitation anomalies (Fig. 3c). Significant negative SST anomalies develop in the North Indian Ocean. Positive SST anomalies in tropical North Pacific displaces eastward. The wind anomalies north of the equator display a pronounced eastward extension over the Philippine Sea and a northward displacement over the North Indian Ocean and the South China Sea. Similar changes are seen in precipitation anomalies. In particular, positive rainfall anomalies dominate over northern South China Sea and rainfall anomalies over southern South China Sea are small.

The SST change in tropical North Pacific appears to be related to surface heat flux anomalies (Wang et al. 2000). Figure 5 shows composite surface net shortwave radiation, latent heat flux, and net surface heat flux anomalies in winter. The downward surface shortwave radiation is reduced over the South China Sea and the Philippine Sea (Fig. 5a) where precipitation and cloud increase (Fig. 3a)

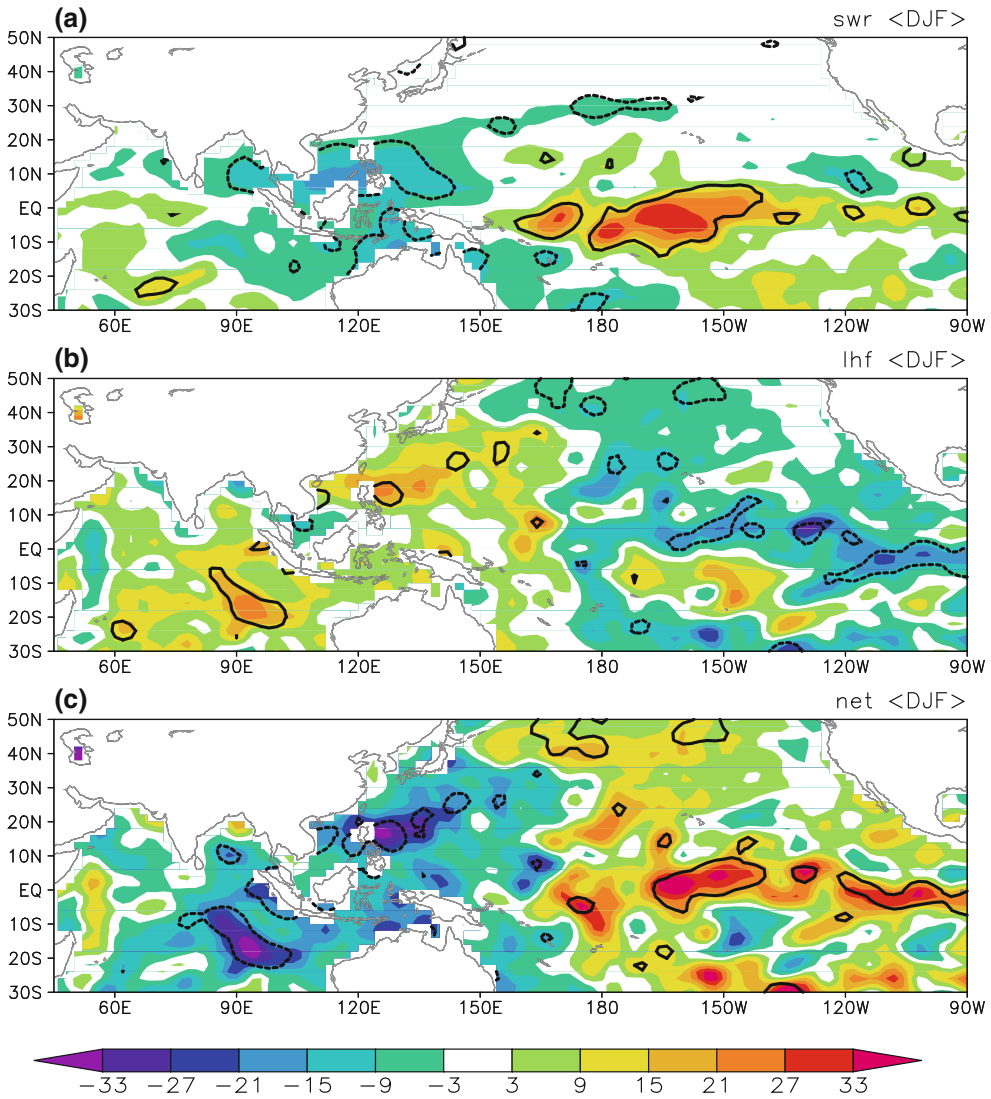

Fig. 5 Composite anomalies of net surface shortwave radiation (positive for downward flux) (**a**), latent heat flux (positive for upward flux) (**b**), and net surface heat flux (positive for downward flux) (**c**) in DJF for ENSO-related winter to summer in-phase relation cases. Thick contours denote regions where the composite anomalies are significant at the 95 % confidence level according to one sample *t* test. The unit is Wm^{-2}

and increases over the equatorial central Pacific where precipitation is suppressed. The upward latent heat flux increases over northern South China Sea and the Philippine Sea (Fig. 5b) where northeasterly anomalous winds enhance surface wind speed (not shown). Over tropical central North Pacific, the latent heat flux decreases. The above surface shortwave radiation and latent heat flux anomalies lead to an east–west contrast of net surface heat flux anomalies with net ocean heat gain over tropical central North Pacific and net ocean heat loss over the South China Sea and the western North Pacific (Fig. 5c). This favors an eastward move of positive SST anomalies.

The SST change in the North Indian Ocean during the decaying phase of ENSO events has been attributed to the ENSO effect through the atmospheric bridge (Klein et al. 1999). El Niño-induced ascent over the North Indian Ocean increases the cloudiness and reduces the shortwave radiation reaching the ocean surface (Klein et al. 1999; Fig. 5a). The associated cyclonic winds enhance surface wind speed and latent heat flux in spring (Figure not shown) when the mean winds turn to westerly. Both shortwave radiation and latent heat flux changes favor the development of negative SST anomalies in summer (Wu et al. 2008; Du et al. 2009; Wu 2009).

One prominent feature in summer is a contrast of SST anomalies between tropical central North Pacific and the North Indian Ocean. The wind and precipitation anomalies over the South China Sea and the Philippine Sea feature a Rossby wave type response to positive SST anomalies in tropical central North Pacific, as pointed out by Wu et al. (2010b, 2011). Numerical experiments with an atmospheric general circulation model (AGCM) showed that local SST anomalies in the western North Pacific can contribute to circulation and convection changes by modulating lower-level convergence and convective instability (Wu and Wang 2000). Several recent studies emphasized the role of the North Indian Ocean SST anomalies in the Philippine Sea anomalous anticyclone during the El Niño decaying phase through a Kelvin wave type response (Yang et al. 2007; Xie et al. 2009; Wu et al. 2009). Thus, it appears that the wind and precipitation anomalies over the South China Sea may be contributed by both positive SST anomalies in tropical North Pacific and negative SST anomalies in the North Indian Ocean, in other words, to an east–west contrast of SST anomalies. Since the SST changes in tropical central North Pacific and the North Indian Ocean are associated with ENSO-induced surface heat flux anomalies, the South China Sea wind and precipitation anomalies in summer can be considered as a delayed response to ENSO.

The influence of the east–west contrast of SST anomalies has been indicated by previous studies. Ohba and Ueda (2006) indicated that the convection around the Philippines in June is sensitive to both the North Indian Ocean SST anomalies and the western North Pacific SST anomalies. Their experiment, however, included the South China Sea SST anomalies that actually result from atmospheric changes. As seen from Fig. 5, the net surface shortwave radiation is reduced significantly over the South China Sea (Fig. 5a) in association with the above-normal precipitation (Fig. 3a). The upward latent heat flux also increases over northern South China Sea (Fig. 5b). Together, there is a net heat loss at the ocean–atmosphere interface (Fig. 5c), leading to SST cooling. As shown by Wu et al. (2006), specification of atmosphere induced SST anomalies in AGCM simulations may force false atmospheric circulation and precipitation anomalies. Through numerical experiments, Wu et al. (2010a) demonstrated that the maintenance of the western North Pacific anomalous anticyclone is contributed by both local SST anomalies and the North Indian Ocean SST anomalies. They concluded that the relative role of in situ and the North Indian Ocean SST anomalies change with month and the role of the western North Pacific SST anomalies weakens in August. One issue with their AGCM experiments is the inclusion of SST anomalies near the Philippines. These SST anomalies, however, are a result of atmospheric change. These regional SST anomalies produce a large anomalous cyclone and associated positive rainfall anomalies in August, which is opposite to observations. Thus, their conclusion about the role of local SST anomalies in August is questionable.

To demonstrate the impact of the east–west contrast of SST anomalies, we conduct idealized numerical experiments with CAM3 model. In the experiments, SST anomalies with a magnitude of 0.5 °C are specified in tropical central North Pacific (9°–21°N, 147.5°–180°E) or the North Indian Ocean (9°–21°N, west to east coast) or both. Our experiments overcome the issue of specifying atmospheric induced SST anomalies in the concerned region, i.e., the South China Sea. Six ensemble model experiments are performed for each of the SST anomalies. The model is integrated from June 1 to August 31 with the initial condition from a control long-term integration with climatological SST specified. In the model integration, the SST anomalies are imposed from June 1-August 31. The 6-ensemble mean difference of experiments with imposed SST anomalies minus the control experiment is considered as the model response to the imposed SST anomalies.

Figure 6 shows the lower-level wind and precipitation anomalies in response to positive SST anomalies in tropical central North Pacific, negative SST anomalies in the North Indian Ocean, and the above SST anomalies in both regions. According to Fig. 6, both the positive SST anomalies in tropical central North Pacific and negative SST anomalies in the North Indian Ocean can induce above-normal precipitation and anomalous cyclonic winds

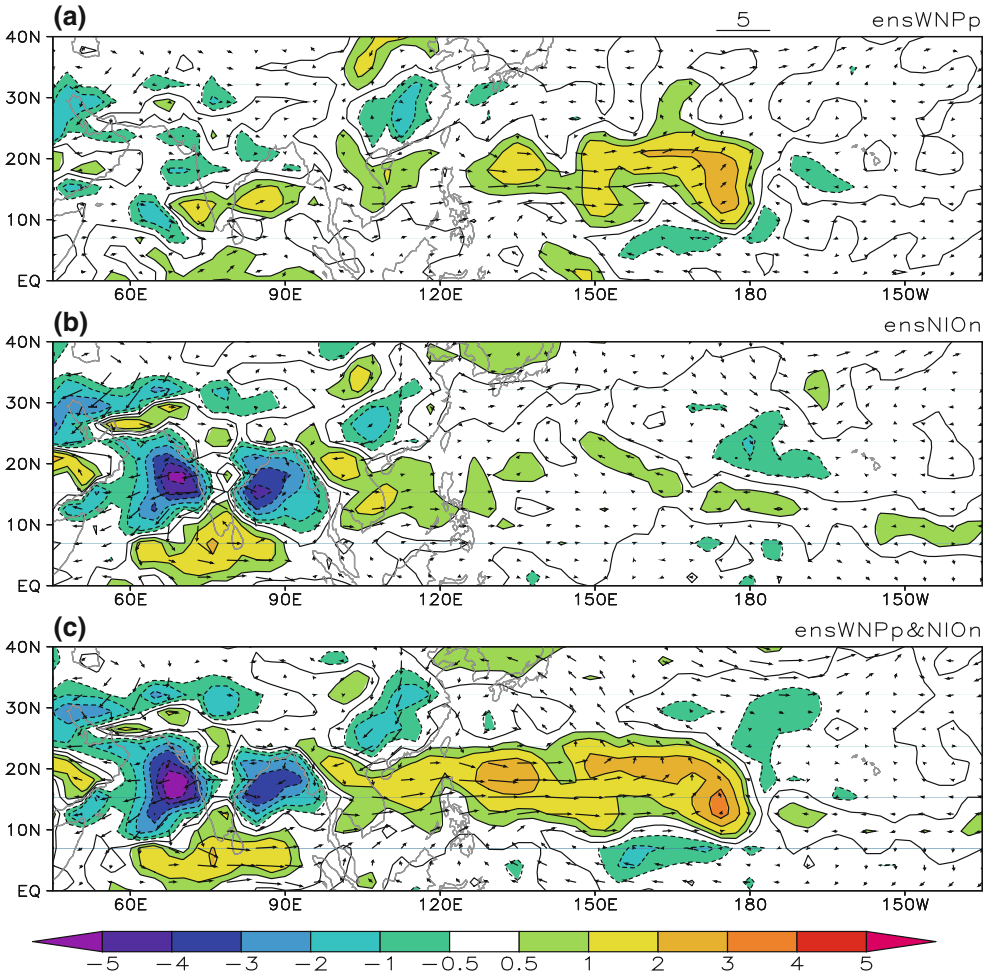

Fig. 6 Response of JJA precipitation (*shading*, unit: mm/day) and 850 hPa winds (*vector*, unit: m/s) to positive SST anomalies of 0.5 °C in the region of 9°–21°N, 147.5°–180°E (**a**), negative SST anomalies of 0.5 °C in the region of 9°–21°N of the North Indian Ocean (**b**), and both (**c**). The wind scale is shown at the top

over northern South China Sea. When opposite SST anomalies are imposed in the above two regions, the wind and precipitation anomalies are much larger. This indicates that opposite SST anomalies in the above two regions can work in cooperation to enhance precipitation anomalies over northern South China Sea. Note that the precipitation response in the model experiments displays differences from observations in northern Bay of Bengal and the equatorial Indian Ocean.

For the four non-ENSO in-phase relation cases from winter to summer, the composite does not show obvious signals in the SST anomaly field (Figures not shown). The individual cases display regional SST anomalies in the western North Pacific and tropical southeastern Indian Ocean during a specific season (winter or summer). This suggests that although regional SST anomalies may contribute to the South China Sea climate variability in individual seasons, the cross-season connection is mostly related to ENSO.

5 Out-of-phase relation from summer to winter

Among the 10 out-of-phase relation cases, 8 cases occurred in years when El Niño or La Niña events develop with the NINO3.4 SST anomalies in the following winter are of the same sign as summer South China Sea precipitation anomalies. The correlation coefficient of the summer leading mode time series with the succeeding winter NINO3.4 SST is +0.37, significant at the 95 % confidence level. Figure 7 shows composite lower-level wind and precipitation anomalies from summer to winter. Figure 8 is similar except for SST anomalies.

In summer, an anomalous cyclone occupies northern South China Sea and the western North Pacific and westerly lower-level wind anomalies extend from eastern Bay of Bengal to the equatorial central Pacific (Fig. 7a). In association, above-normal precipitation appears over northern South China Sea and the western North Pacific, whereas below-normal precipitation is seen over the

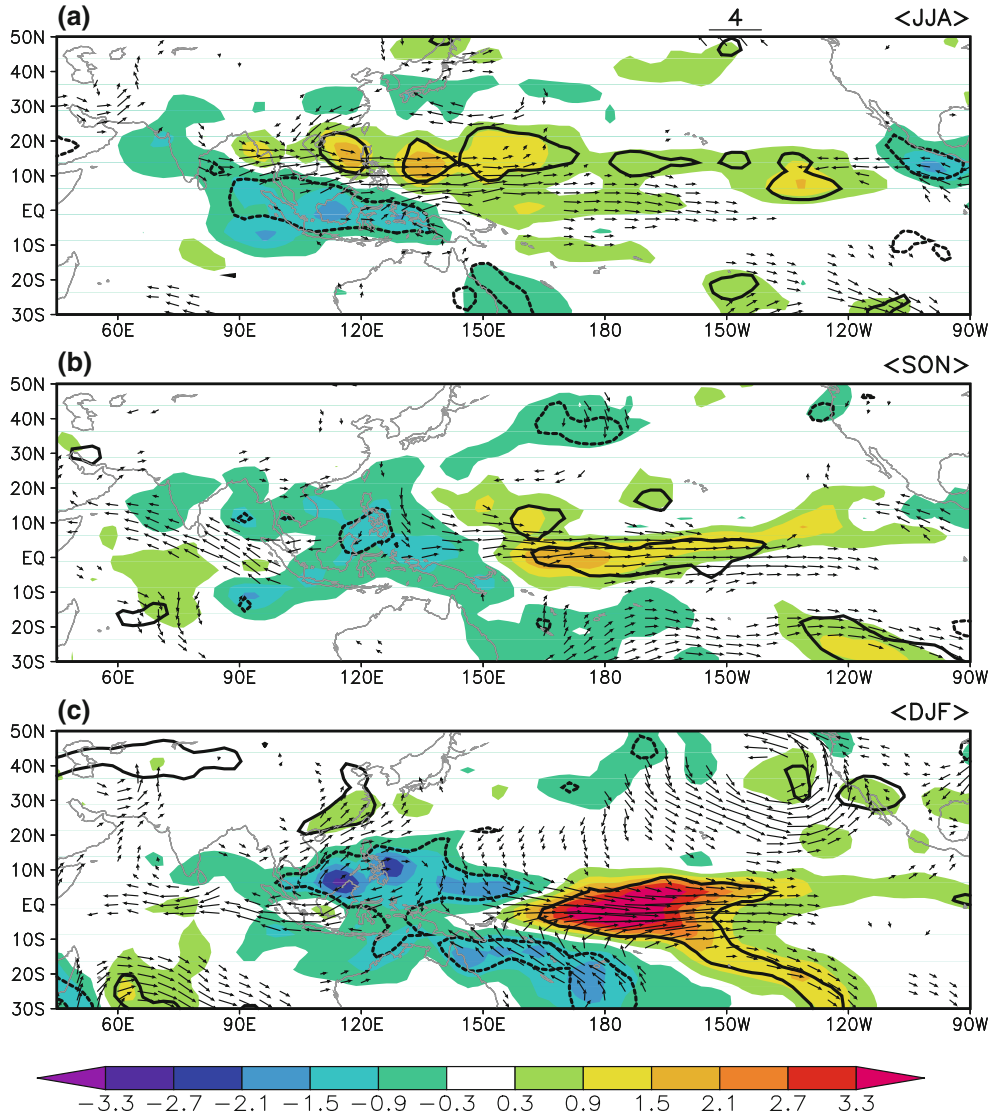

Fig. 7 Composite anomalies of precipitation (*shading*, unit: mm/day) and 850 hPa wind (*vector*, unit: m/s) in JJA (**a**), SON (**b**), and DJF (**c**) for summer to winter out-of-phase relation cases. The wind scale is shown at the top. Thick contours denote regions where the composite precipitation anomalies are significant at the 95 % confidence level according one sample *t* test. Only wind anomaly vectors that are significant at the 95 % confidence level are shown

Maritime Continent. These wind and precipitation anomalies feature a Rossby wave type response to positive SST anomalies in the equatorial central and eastern Pacific (Fig. 8a). The anomalous cyclone features a large westward extension, which may indicate a contribution of anomalous atmospheric cooling over the Maritime Continent via an anomalous Hadley type circulation. In turn, suppressed precipitation over the Maritime Continent may be attributed to positive SST anomalies in the equatorial central Pacific via an anomalous Walker circulation (Wang et al. 2003).

In fall, westerly wind anomalies and above-normal precipitation control the equatorial central Pacific (Fig. 7b). The region of below-normal precipitation expands from the Maritime Continent to the Bay of Bengal, the South China Sea, and the Philippine Sea. Anticyclonic wind anomalies develop over the North Indian Ocean and the South China Sea. These wind and precipitation anomalies can be attributed to positive SST anomalies in the equatorial central and eastern Pacific (Fig. 8b). On one hand, the positive SST anomalies induce westerly wind anomalies and above-normal precipitation over the equatorial central Pacific through a Gill type response. On the other hand, the associated anomalous heating induces compensating downward motion and anomalous cooling over the Maritime Continent that, in turn, leads to below-normal precipitation and anomalous anticyclone to the northwest through a Rossby wave type response.

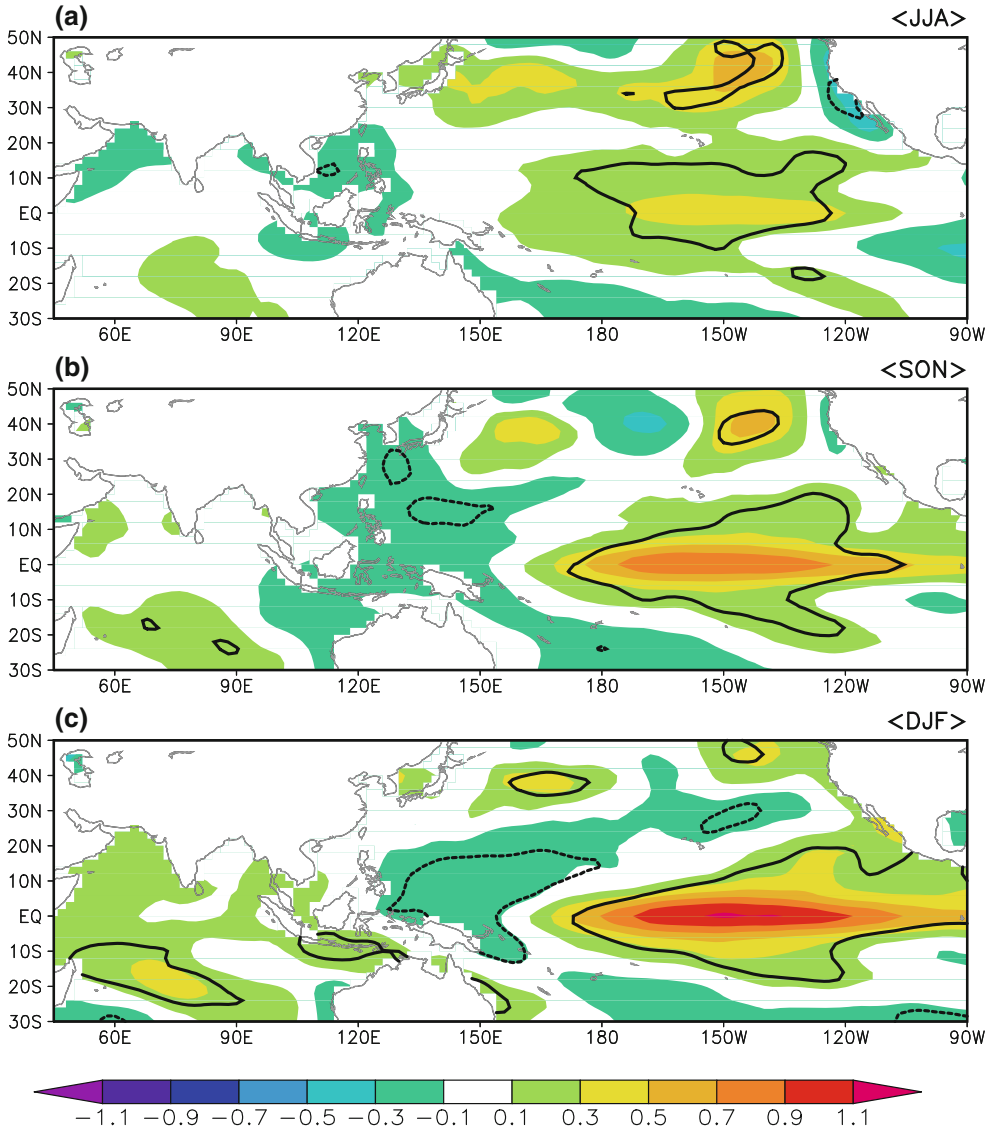

Fig. 8 Composite anomalies of SST (°C) in JJA (**a**), SON (**b**), and DJF (**c**) for summer to winter out-of-phase relation cases. Thick contours denote regions where the composite SST anomalies are significant at the 95 % confidence level according one sample *t* test

In winter, following a further increase in the positive SST anomalies in the equatorial central and eastern Pacific (Fig. 8c), both precipitation and wind anomalies intensify over the tropics (Fig. 7c). In addition, wind and precipitation anomalies move eastward both north and south of the equator over the Indian Ocean and the western Pacific. At this time, southern South China Sea is under the influence of significant negative precipitation and anticyclonic wind anomalies. In addition to positive SST anomalies in the equatorial central and eastern Pacific, significant negative SST anomalies develop in tropical western Pacific (Fig. 8b, c). These negative SST anomalies may contribute to precipitation and wind anomalies over the South China Sea and the Philippine Sea through a Rossby wave type response (Wang et al. 2000) and through modulating the lower-level moisture convergence and convective instability (Wu and Wang 2000). Thus, both positive SST anomalies in the equatorial central Pacific and negative SST anomalies in tropical western North Pacific appear to contribute to precipitation and wind anomalies over the South China Sea and the Philippine Sea.

The development of the negative SST anomalies in tropical western North Pacific appears to be associated with atmospheric changes. The positive rainfall anomalies in summer over the Philippine Sea are accompanied by a reduction of downward shortwave radiation reaching the ocean surface (Fig. 9a). The anomalous westerly winds enhance the surface wind speed, leading to an increase in upward surface latent heat flux over southern Philippine Sea (Fig. 9b). Together, these induce a net surface heat loss

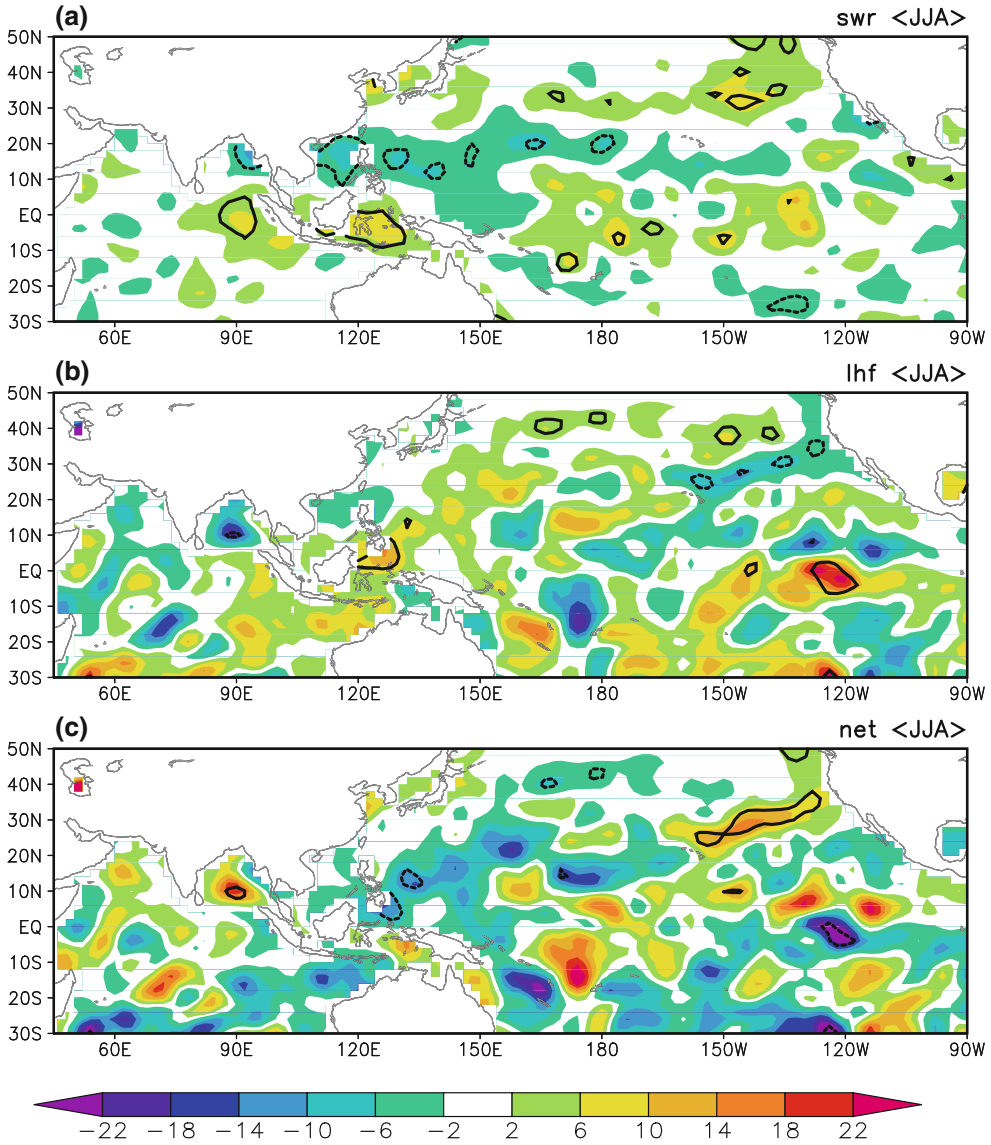

Fig. 9 Composite anomalies of net surface shortwave radiation (positive for downward flux) (**a**), latent heat flux (positive for upward flux) (**b**), and net surface heat flux (positive for downward flux) (**c**) in JJA for summer to winter out-of-phase relation cases. Thick contours denote regions where the composite anomalies are significant at the 95 % confidence level according to one sample *t* test. The unit is Wm^{-2}

over the Philippine Sea, leading to SST cooling. Thus, an atmosphere–ocean interaction process operates over tropical western North Pacific during the out-of-phase relation from summer to winter. Lestari et al. (2011) indicated a similar atmospheric forcing of SST changes in the South China Sea during strong monsoon years.

The above interaction feature is further demonstrated using Fig. 10 that shows temporal evolution of area-mean anomalies. Accompanying positive precipitation anomalies in summer, net surface shortwave radiation reduces over the Philippine Sea (Fig. 10a). At the same time, surface evaporation enhances in association with the increase in surface wind speed over southern Philippine Sea. Together, the ocean loses heat through surface heat fluxes (Fig. 10b). As a result, the SST decreases and turns from positive in spring to negative in fall and winter in southern Philippine Sea (Fig. 10b). The negative SST anomalies maintain to winter, followed by intensified precipitation decrease in winter over southern South China Sea.

6 Summary and discussions

The present study documents the cross-season connections of rainfall variability between winter and summer in the South China Sea region. Analysis of observations shows

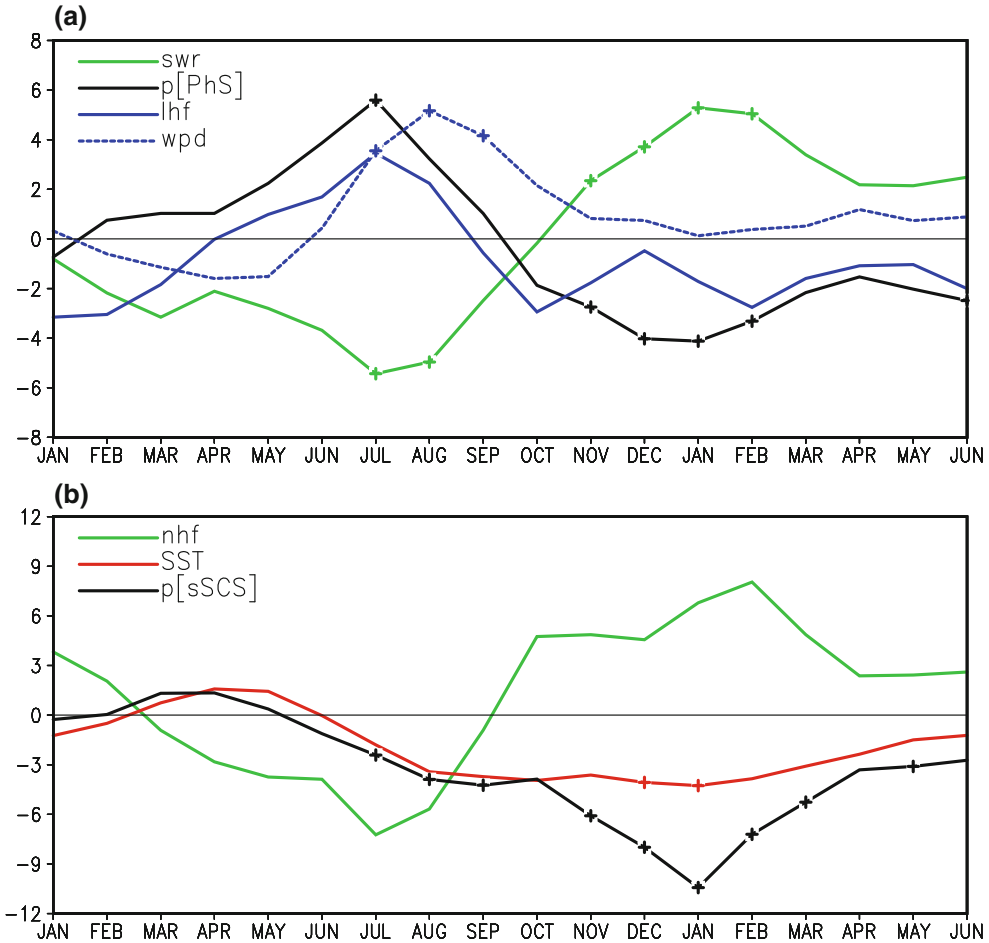

Fig. 10 Area-mean anomalies of net surface shortwave radiation (Wm^{-2}) and precipitation (mm/day) over the region of 10°–20°N, 120°–150°E, surface latent heat flux (Wm^{-2}) and wind speed (m/s) over the region of 5°–15°N, 120°–150°E (**a**), net surface heat flux (Wm^{-2}) and SST (°C) over the region of 5°–15°N, 120°–150°E and precipitation (mm/day) over the region of 2.5°–12.5°N, 107.5°–117.5°E (**c**). Marked points denote anomalies significant at the 95 % confidence level according to one sample *t* test. In the plot, precipitation, wind speed, and SST anomalies have been multiplied by 5, 10, and 20, respectively

that there is a tendency for above-normal rainfall over southern South China Sea in boreal winter to be followed by above-normal rainfall over northern South China Sea in boreal summer. This winter-to-summer connection is denoted as in-phase relation. Furthermore, above-normal rainfall over northern South China Sea in boreal summer tends to be succeeded by below-normal rainfall over southern South China Sea in the following winter. This summer-to-winter connection is denoted as out-of-phase relation. The above cross-season connections of rainfall anomalies provide a source of predictability for rainfall in the South China Sea region.

The in-phase relation from winter to summer tends to occur in the El Niño/La Niña decaying years. During the mature phases of El Niño/La Niña events, anomalous heating/cooling over the equatorial central Pacific induces anomalous descent/ascent over southern South China Sea, leading to decrease/increase in rainfall there. In the following summer, positive/negative SST anomalies in the North Indian Ocean and negative/positive SST anomalies in tropical central North Pacific develop in response to ENSO induced surface heat flux changes, forming an east–west contrast. The SST anomalies in the above two regions operate together through Kelvin wave and Rossby wave type responses, suppressing/enhancing rainfall over northern South China Sea. Thus, these regional SST anomalies act as a medium for a delayed impact of ENSO on the South China Sea summer rainfall. The combined effects of tropical central North Pacific and the North Indian Ocean SST anomalies are confirmed by numerical experiments with an AGCM.

The out-of-phase relation from summer to winter tends to occur in the El Niño/La Niña developing years. In summer, positive/negative SST anomalies in the equatorial central Pacific induce an anomalous cyclone/anticyclone that extends to northern South China Sea, enhancing/suppressing rainfall there. Accompanying the maturing of El Niño/La Niña events, anomalous descent/ascent reduces/

enhances rainfall over southern South China Sea in winter. The accompanying negative/positive SST anomalies in the western North Pacific also contribute to the decrease/increase of rainfall over southern South China Sea.

Analysis indicates that there is an air-sea interaction process in the Philippine Sea region. Above-normal precipitation and enhanced wind increase the surface heat loss during summer and fall, cooling down the SST in the Philippine Sea. The lower SST, in turn, contributes to the decrease of rainfall over southern South China Sea through a Rossby wave type response in winter. This air-sea interaction process provides a delayed impact of ENSO on the South China Sea climate variability.

The present study focuses on the in-phase relation from winter to summer and the out-of-phase relation from summer to winter. As listed in Table 1, there are cases of opposite rainfall anomalies between winter and summer as well as cases of same sign rainfall anomalies between summer and the following winter. Some of these cases are El Niño/La Niña years. For example, out-of-phase relation cases from winter to summer in 1995, 1995, 2005, 2006, and 2007 are El Niño/La Niña decaying years; in-phase relation cases from summer to winter in 1988, 1995, and 2005 are El Niño/La Niña developing years. These suggest that ENSO decaying (developing) years are not always accompanied by in-phase (out-of-phase) relation from winter to summer (from summer to winter).

To understand why the above ENSO decaying (developing) years are not followed by in-phase (out-of-phase) relation, we have compared the composite SST anomalies in these cases with those in Figs. 4, 8. For the out-of-phase relation cases from winter to summer, one feature to note is that the SST anomalies in the North Indian Ocean and tropical central North Pacific are weak in summer (Figure not shown). This feature is also observed in individual cases. This result appears to support the role of regional SST anomalies in the above regions in relating ENSO to summer South China Sea rainfall variability and thus the in-phase relation from winter to summer. For the in-phase relation from summer to winter, significant positive SST anomalies are maintained in the equatorial western North Pacific (Figure not shown), which are opposite to those in Fig. 8c. These positive SST anomalies appear to induce positive rainfall anomalies in southern South China Sea in winter via a Rossby wave type response. This result supports the important role of the regional SST anomalies in the equatorial western North Pacific in the summer to winter connection of the South China Sea rainfall anomalies.

Acknowledgments This study is supported by the Direct Grants of the Chinese University of Hong Kong (2021105), the Hong Kong Research Grant Council grant (CUHK#403612), and the National Natural Science Foundation of China grants (41275081 and 41295049).

References

Adler RF, Huffman GJ, Chang A, Ferraro R, Xie P, Janowiak J, Rudolf B, Schneider U, Curtis S, Bolvin D, Gruber A, Susskind J, Arkin P (2003) The version 2 global precipitation climatology project (GPCP) monthly precipitation analysis (1979-present). J Hydrometeor 4:1147–1167

Berry DI, Kent EC (2009) A new air–sea interaction gridded datasets from ICOADS with uncertainty estimates. Bull Amer Meteor Soc 90:645–656

Collins WD, Bitz CM, Blackmon ML, Bonan GB, Bretherton CS, Carton JA, Chang P, Doney SC, Hack JJ, Henderson TB, Kiehl JT, Large WG, McKenna DS, Santer BD, Smith RD (2006) The community climate system model version 3 (CCSM3). J Climate 19:2122–2143

Du Y, Xie SP, Huang G, Hu K (2009) Role of air–sea interaction in the long persistence of El Niño–induced North Indian Ocean warming. J Climate 22:2023–2038

Kanamitsu M, Ebisuzaki W, Woollen J, Yang SK, Hnilo JJ, Fiorino M, Potter GL (2002) NCEP–DOE AMIP-II Reanalysis (R-2). Bull Amer Meteor Soc 83:1631–1643

Klein SA, Sode BJ, Lau NC (1999) Remote sea surface temperature variations during ENSO: evidence for a tropical atmospheric bridge. J Climate 12:917–932

Lestari RK, Watanabe M, Kimoto M (2011) Role of air-sea coupling in the interannual variability of the South China Sea summer monsoon. J Meteor Soc Japan 89A:283–290

North GR, Bell TL, Cahalan RF, Moeng FJ (1982) Sampling errors in the estimation of empirical orthogonal functions. Mon Wea Rev 110:699–706

Ohba M, Ueda H (2006) A role of zonal gradient of SST between the Indian Ocean and the western Pacific in localized convection around the Philippines. SOLA 2:176–179

Smith TM, Reynolds RW, Peterson TC, Lawrimore J (2008) Improvements to NOAA's historical merged land–ocean surface temperature analysis (1880–2006). J Climate 21:2283–2296

Tomita T, Yasunari T (1996) Role of the northeast winter monsoon on the biennial oscillation of the ENSO/monsoon system. J Meteor Soc Japan 74:399–413

Wang B, Wu R, Fu X (2000) Pacific-East Asian teleconnection: how does ENSO affect East Asian climate? J Climate 13:1517–1536

Wang D, Xie Q, Du Y, Wang WQ, Chen J (2002) The 1997–1998 warm event in the South China Sea. Chinese Sci Bull 47:1221–1227

Wang B, Wu R, Li T (2003) Atmosphere-warm ocean interaction and its impacts on Asian-Australian monsoon variation. J Climate 16:1195–1211

Wang C, Wang W, Wang D, Wang Q (2006) Interannual variability of the South China Sea associated with El Niño. J Geophys Res 111:C03023. doi:10.1029/2005JC003333

Wu R (2009) Possible role of the Indian Ocean in the out-of-phase transition of the Australian to Indian summer monsoon. J Climate 22:1834–1849

Wu R, Wang B (2000) Interannual variability of summer monsoon onset over the western North Pacific and the underlying processes. J Climate 113:2483–2501

Wu R, Hu ZZ, Kirtman BP (2003) Evolution of ENSO-related rainfall anomalies in East Asia. J Climate 16:3742–3758

Wu R, Kirtman BP, Pegion K (2006) Local air-sea relationship in observations and model simulations. J Climate 19:4914–4932

Wu R, Kirtman BP, Krishnamurthy V (2008) An asymmetric mode of tropical Indian Ocean rainfall variability in boreal spring. J Geophys Res 113:D05104. doi:10.1029/2007JD009316

Wu B, Zhou T, Li T (2009) Seasonally evolving dominant interannual variability modes of East Asian climate. J Climate 22:2992–3005

Wu B, Li T, Zhou T (2010a) Relative contributions of the Indian Ocean and local SST anomalies to the maintenance of the western North Pacific anomalous cyclone during El Niño decaying summer. J Climate 23:2974–2986

Wu R, Yang S, Liu S, Sun L, Lian Y, Gao ZT (2010b) Changes in the relationship between Northeast China summer temperature and ENSO. J Geophys Res 115:D21107. doi:10.1029/2010JD014422

Wu R, Yang S, Liu S, Sun L, Lian Y, Gao ZT (2011) Northeast China summer temperature and North Atlantic SST. J Geophys Res 116:D16116. doi:10.1029/2011JD015779

Wu R, Yang S, Wen ZP, Huang G, Hu K (2012) Interdecadal change in the relationship of southern China summer rainfall with tropical Indo-Pacific SST. Theor Appl Climatol 108:119–133. doi:10.1007/s00704-011-0519-4

Xie SP, Xie Q, Wang D, Liu WT (2003) Summer upwelling in the South China Sea and its role in regional climate variations. J Geophys Res 108:3261. doi:10.1029/2003JC001867

Xie SP, Hu K, Hafner J, Tokinaga H, Du Y, Huang G, Sampe T (2009) Indian Ocean capacitor effect on Indo-western Pacific climate during the summer following El Niño. J Climate 22: 730–747

Yang JL, Liu QY, Xie SP, Liu ZY, Wu LX (2007) Impact of the Indian Ocean SST basin mode on the Asian summer monsoon. Geophys Res Lett 34:L02708. doi:10.1029/2006GL028571

Zhou LT, Tam CY, Zhou W, Chan JCL (2010) Influence of South China Sea SST and ENSO on winter rainfall over South China. Adv Atmos Sci 27(4):832–844. doi:10.1007/s00376-009-9102-7